ETV4-mediated transcriptional activation of SLC12A5 exacerbates ferroptosis resistance and glucose metabolism reprogramming in breast cancer cells

HUAN WANG, YANYAN DAI and FENGXIANG WANG

Department of Pathology, Wenzhou Central Hospital, Wenzhou, Zhejiang 325000, P.R. China

Received January 18, 2024; Accepted May 20, 2024

DOI: 10.3892/mmr.2024.13341

Abstract. Solute carrier family 12 member 5 (SLC12A5) is an oncogene in numerous types of cancer, however its function in breast cancer (BC) remains elusive. ETS translocation variant 4 (ETV4) promotes BC. Therefore, the present study aimed to elucidate the role of SLC12A5 in ferroptosis and glucose metabolism in BC cells as well as to understand the underlying mechanism. Analysis of data from the UALCAN database demonstrated expression levels of SLC12A5 in BC and its association with prognosis. Reverse transcription-quantitative PCR and western blotting were conducted to evaluate the expression levels of SLC12A5 and ETV4 in BC cells. The abilities of BC cells to proliferate, migrate and invade were assessed using Cell Counting Kit-8, colony formation, wound healing and Transwell assays. Thiobarbituric acid reactive substances assay and a C11 BODIPY 581/591 probe were used to evaluate lipid peroxidation. Ferroptosis resistance was evaluated by the measurement of Fe^{2+} and ferroptosis-related solute carrier family 7a member 11 (SLC7A11), glutathione peroxidase 4 (GPX4), acyl-CoA synthetase long-chain family member 4 (ACSL4) and transferrin receptor 1 (TFR1) protein levels. Glycolysis was assessed via evaluation of extracellular acidification rate, oxygen consumption rate, lactate production and glucose consumption. Finally, luciferase reporter and chromatin immunoprecipitation assay were used to verify the interaction between ETV4 and the SLC12A5 promoter. UALCAN database analysis indicated that SLC12A5 was upregulated in BC tissues and cells and that SLC12A5 elevation indicated a poor prognosis of patients with BC. SLC12A5 knockdown suppressed the BC cell proliferative, migratory and invasive capabilities. Moreover, SLC12A5 knockdown decreased BC cell ferroptosis resistance and glucose metabolism reprogramming. The transcription factor ETV4 was demonstrated to bind to the SLC12A5 promoter and upregulate its transcription. Furthermore, ETV4 overexpression counteracted the suppressive effect of SLC12A5 knockdown on the BC cell proliferative, migratory and invasive abilities, as well as on ferroptosis resistance and glucose metabolism reprogramming. Transcriptional activation of SLC12A5 by ETV4 modulated the migration, invasion, ferroptosis resistance and glucose metabolism reprogramming of BC cells.

Correspondence to: Dr Fengxiang Wang, Department of Pathology, Wenzhou Central Hospital, 252 Baili East Road, Lucheng, Wenzhou, Zhejiang 325000, P.R. China
E-mail: wangfxdoc021@163.com

Key words: solute carrier family 12 member 5, breast cancer, ETS translocation variant 4, ferroptosis, glucose metabolism reprogramming

Introduction

Breast cancer (BC) is a prevalent tumor that threatens the lives and health of patients (1). The latest global cancer statistics indicated that 310,720 female patients were diagnosed with BC in 2024 in the United States (2). Globally, BC remains the most common type of malignancy in female patients, with at least 500,000 BC-associated mortalities each year. In recent years, with changes in lifestyle and environment, the incidence of BC is increasing year by year, and the onset age is becoming younger (3). Although early diagnosis and novel treatment methods such as surgery, postoperative chemotherapy and hormone and targeted therapy have rapidly progressed, the prevalence and mortality rates of BC remain high with the 5-year survival rate of patients with metastatic BC <30% (4-6). Moreover, certain patients still encounter rapid tumor progression following treatment and exhibit a poor prognosis (7). Therefore, it is key to evaluate novel and reliable molecular markers and therapeutic targets for BC treatment.

Ferroptosis is a non-apoptotic form of regulated cell death characterized by iron dependency and lipid peroxidation (8). When the levels of intracellular iron ions increase, the production of lipid reactive oxygen species (ROS) also increases. GPX4 is required to maintain the balance between ROS production and clearance; when this is not sustained, ferroptosis occurs (9). System Xc is an antioxidant system widely distributed in the phospholipid bilayer, composed of two SLC7A11 subunits and a SLC3A2 heterodimer (10). Increases in SLC7A11 and GPX4 inhibit occurrence of ferroptosis. Moreover, circulating iron binds to TF in the form of Fe^{3+} and enters the cell via TFR1. ACSL4 is required for ROS accumulation, so elevated levels of TFR1 and ACSL4 promote ferroptosis (11). Emerging studies have shown that ferroptosis

pathway can repress tumor growth and kill tumor cells, which may be a new idea for antitumor treatment (9,11). In particular, ferroptosis is closely involved in the development of BC (12).

Solute carrier family 12 member 5 (SLC12A5) is primarily responsible for transporting chloride ions in and out of the cell and serves a role in regulating cell volume (13). Initially, researchers focused on the role of SLC12A5 in the nervous system and it was reported that SLC12A5 is upregulated in glioblastoma, where it enhances chloride ion transport ability of glioma cells and facilitates alteration of cell size and morphology as well as metastasis (14). With advancement of biological research, further studies reported that SLC12A5 is upregulated in a number of types of cancer and that SLC12A5 upregulation promotes numerous tumor characteristics and indicates poor patient prognosis (14-17). A previous study reported that increased levels of SLC12A5 are associated with poor prognosis in patients with hepatocellular carcinoma (HCC) and SLC12A5 inhibits ferroptosis in HCC to promote tumorigenesis through upregulating expression of the cystine transporter xCT (18). Moreover, SLC12A5 is highly expressed in human bladder tumors and linked to poor survival in patients with uroepithelial carcinoma of the bladder. Upregulation of SLC12A5/SRY-box transcription factor 18 facilitates tumor invasion and metastasis (19). Furthermore, SLC12A5 is amplified, which is accompanied with the concurrent amplification of an 8-gene Signature (TNF-α, IL-1β, IL-6, MMP1, MMP9, TGF-β1, TGF-βRII, EGFR) derived based on these macrophage-tumor interactions in BC (20).

Avian erythroblastosis virus E-26 transformation specific (ETS) translocation variant 4 (ETV4) is a member of the PEA3 subfamily of ETS transcription factor (21). PEA3 subfamily influences cancer progression and metastasis by regulating cell cycle, apoptosis, epithelial-mesenchymal transition, cell migration and invasion, development of cancer stem cell phenotypes and chemotherapy resistance (22). ETV4 gene is located on chromosome 17q21 and binds to adenovirus E1A enhancer element. ETV4 has a highly conserved 85-amino acid ETS domain that binds to DNA, thus ETV4 can modulate expression of genes which regulate the proliferation and metastasis of cancer cells (23). Moreover, ETV4 has been reported to enhance glycolytic activity and stemness in BC (24). ETV4 controls HK1 expression and glycolysis-lactate production to activate mTORC1 by relieving Tuberous sclerosis complex 2 (TSC2) repression of Ras homolog enriched in brain (Rheb) in non-small cell lung cancer cells by regulating glycolysis-lactate production (25). However, to the best of our knowledge, expression of SLC12A5 and ETV4 in BC and their role in the development of BC remains unclear. Therefore, the present study aimed to assess the role of SLC12A5 in BC and clarify the mechanism underlying its effects in this disease.

Materials and methods

Bioinformatics analysis. SLC12A5 gene expression in the tissue of patients with BC and the association of SLC12A5 with poor prognosis in these patients were analyzed using the University of ALabama at Birmingham CANcer data analysis Portal (UALCAN) database (ualcan.path.uab.edu) from TCGA database (26). The binding site of ETV4 and the SLC12A5 promoter was predicted using HumanTFDB database (bioinfo.life.hust.edu.cn/HumanTFDB/#!/, version 3.0 (27). Moreover, expression of SLC12A5 in BC cell lines was analyzed by Cancer Cell Line Encyclopedia (CCLE) project (depmap.org/portal/ccle/) (28).

Cell lines. The human normal mammary epithelial cell line MCF10A and BC cell lines MCF-7, Hs578T, T47D and BT-549 were purchased from Cellverse Bioscience Technology Co., Ltd. MCF10A cells were cultured in DMEM/F12 with L-glutamine and 5% horse serum (Thermo Fisher Scientific, Inc.), 20 ng/ml epidermal growth factor, 0.5 μg/ml hydrocortisone, 100 ng/ml cholera toxin and 10 μg/ml insulin (all Gibco; Thermo Fisher Scientific, Inc.) and 1% penicillin/streptomycin (1:100; Thermo Fisher Scientific, Inc.) at 37˚C with 5% CO_2. BC cell lines were cultivated in DMEM (Thermo Fisher Scientific, Inc.) supplemented with 10% fetal bovine serum (FBS; Gibco; Thermo Fisher Scientific, Inc.) and 1% penicillin-streptomycin at 37˚C with 5% CO_2.

Cell transfection. ETV4-overexpressing plasmid were constructed by inserting the ETV4 coding sequence into a pcDNA3.1 plasmid (General Biosystems, Inc.). An empty pcDNA3.1 vector was used as the negative control (oe-NC). The specific short hairpin (sh)RNA sequences targeting SLC12A5 (sh-SLC12A5-1, 5'-GCAATGCAATGAAGT TGAA-3' and sh-SLC12A5-2, 5'-GGAGAGGTTGCAAAC CAAA-3'), ETV4 (sh-ETV4-1, 5'-GGTGGTGATCAAACA GGAA-3' and sh-ETV4-2, 5'-GGAATGGAGTTCAAGCTC A-3'), negative control (sh-NC, 5'-CCGGCAACAAGATGA AGAGCACCAACTC-3') were cloned into the pLKO.1-puro vector (Sigma, St. Louis, USA). An empty pLKO.1-puro vector was used as the control. These plasmids and shRNAs were constructed by Shanghai GenePharma Co., Ltd. A total of 5 μg plasmid or 5 μg shRNA was transfected into MCF7 cells using Lipofectamine 2000 (Invitrogen; Thermo Fisher Scientific, Inc.) at 37˚C for 48 h, according to the manufacturer's instructions. After culturing for 2 days at 37˚C, cells were used for the following experiments. Untransfected cells were referred to as the Control group.

Cell Counting Kit-8 (CCK-8) assay. MCF-7 cells were seeded in 96-well plates at $3x10^3$ cells/well and incubated for 24, 48 and 72 h at 37˚C with 5% CO_2 and saturated humidity. Subsequently, 10 μl of CCK-8 solution (Beijing Solarbio Science & Technology Co., Ltd.) was added to each well and incubated for 1 h. The OD value at 450 nm was then measured using a microplate reader (Biochrom, Ltd.).

Colony formation assay. Transfected MCF-7 cells were inoculated into 6-well plates (500 cells/well). Following a 2-week incubation in DMEM with 10% FBS at 37˚C, the cells were fixed with 4% paraformaldehyde at room temperature for 25 min and stained with 0.1% crystal violet for 10 min at room temperature. Colonies (>50 cells) were counted manually in five fields of view using a light microscope (Olympus Corporation; magnification, x10). Each group was replicated for five times.

Wound healing assay. MCF-7 cells transfected with sh-SLC12A5 in the presence or absence of oe-ETV4 or oe-NC were seeded into 6-well plates at $5x10^5$ cells/well and incubated in DMEM with 10% FBS at 37˚C until 90% confluency was reached. A straight scratch in the cell monolayer was made to create a denuded zone using a pipette tip. The cells were then incubated for 24 h in serum-free DMEM medium and images of the wound surface and number of migrated cells were captured under an inverted microscope (Olympus Corporation; magnification, x100). Five fields were randomly chosen and analyzed in each well. The relative migration rate was calculated as follows: (wound width at 0 h-wound width at 24 h)/wound width at 0 h x100.

Transwell assay. MCF-7 cells were collected and suspended at a final concentration of $2x10^5$ cells/ml in serum-free DMEM (Thermo Fisher Scientific, Inc.). A total of 200 μl cell suspension was transferred to the upper wells of Transwell chambers (Corning, Inc.) coated with 0.1 ml Matrigel (Becton, Dickinson and Company) at 37˚C for 1 h and DMEM containing 10% FBS was placed in the lower chamber. Following 24 h incubation at 37˚C, a cotton swab was used to remove cells in the upper chamber, while cells in the lower chamber were fixed with 100% methanol at room temperature for 10 min and stained with 0.5% crystal violet for 10 min at room temperature. Finally, a light microscope (Olympus Corporation; magnification x100) was used for cell counting. Five randomly chosen fields were counted for each group.

Measurement of lipid peroxidation. Thiobarbituric acid reactive substances (TBARS) assay was performed to estimate lipid peroxidation in MCF-7 cells. For this, 7 μl 500 mM butylated hydroxyanisole and 0.25 ml 15% (w/v) trichloroacetic acid were added to the cell lysate, which was centrifuged at 1,000 x g for 5 min at 4˚C. The supernatant was collected and 0.5 ml 0.375% (w/v) TB was added. After 10 min boiling at 95˚C, the levels of TBARS were estimated using a microplate reader (Thermo Fisher Scientific, Inc.) at 532 nm.

BODIPY 581/591 C11 probe (Thermo Fisher Scientific, Inc.) was also used to detect lipid peroxidation. Transfected MCF-7 cells were incubated with 10 μM C11 BODIPY 581/591 probe for 10 min at 37˚C. The presence of green fluorescence indicated oxidized probe; red fluorescence indicated non-oxidized probe. ImageJ (version 1.8.0; National Institutes of Health) was used to assess the levels of BODIPY 581/591 C11, calculated as the ratio of green fluorescence/total fluorescence.

Detection of Fe^{2+} levels. MCF-7 cells were transfected with sh-SLC12A5 in the presence or absence of oe-ETV4 or oe-NC. Fe^{2+} levels were measured using an Iron Assay kit purchased from Abcam (cat. no. ab83366) at 593 nm, according to the manufacturer's instructions.

Extracellular acidification rate (ECAR) analysis. XF96 Extracellular Flux Analyzer (Agilent Technologies, Inc.) with Seahorse XFp Glycolysis Stress Test kit (Agilent Technologies, Inc.) was used to measure ECAR in MCF-7 cells. Transfected MCF-7 cells were inoculated into wells of the Seahorse XF plate at $1x10^4$ cells/well and exposed to glucose (1 μM), oligomycin (1 μM) and 2-deoxyglucose (500 mM) at 37˚C for 1 h. Finally, the results were analyzed by Seahorse XF96 Wave software (version 2.6; Seahorse Bioscience; Agilent Technologies) and ECAR was calculated as mpH/min.

Evaluation of oxygen consumption rate (OCR). The OCR was measured using a Seahorse XF Cell Mito Stress Test kit (cat. no. 103010-100; Seahorse Bioscience; Agilent Technologies, Inc). The sensor cartridge of the XFp analyzer was calibrated for 24 h in a non-CO_2 incubator at 37˚C. Cells were cultured in XFp cell culture plates at 5,000 cells/well at 37˚C for 24 h. After transfection, MCF-7 cells were incubated in 180 μl assay medium (XF Base Medium, 1 mM pyruvate, 5.5 mM glucose and 2 mM L-glutamine, pH 7.4) for 1 h at 37˚C in a non-CO_2 incubator, according to the manufacturer's protocol. The results were analyzed by Seahorse XF96 Wave software (version 2.6; Seahorse Bioscience; Agilent Technologies).

Measurement of lactate production and glucose consumption. MCF-7 cells were transfected with sh-SLC12A5 in the presence or absence of oe-ETV4. Cells were cultured for 24 h at 37˚C and the cell medium was collected for lactate and glucose measurement using Lactate Assay Kit (cat. no. MAK064; Sigma-Aldrich; Merck KGaA) and Glucose Assay kit (cat. no. MAK476; Sigma-Aldrich; Merck KGaA), respectively according to the manufacturer's instructions.

Dual-luciferase reporter assay. Activity of SLC12A5 promoter was evaluated using a dual-luciferase reporter assay. Briefly, SLC12A5 promoter fragments including the wild-type (WT) or mutant (MUT) target sites for ETV4 were cloned into the pGL3-Control vector (Promega Corporation) to create the reporter vectors SLC12A5-WT or SLC12A5-MUT, respectively (Data S1). Luciferase reporter vectors and oe-NC or oe-ETV4 were co-transfected into MCF-7 cells for 48 h at 37˚C using Lipofectamine 2000. After 48 h incubation at 37˚C, Dual-Luciferase Reporter Assay (Promega Corporation) was used for estimation of relative luciferase activities; luciferase activity was normalized to Renilla.

Chromatin immunoprecipitation (ChIP) assay. MCF-7 Cells were cross-linked with 1% formaldehyde for 10 min at 37˚C, then quenched with 2.5 M glycine at room temperature for 5 min. Subsequently, cells were harvested by centrifugation at 300 x g for 3 min at room temperature, washed with PBS, and lysed in SDS lysis buffer (Upstate Biotechnology, Inc.), and the chromatin from the cell lysates was sonicated with a 10-sec on and 10-sec off mode for 12 cycles on ice to shear DNA into fragments at 20 kHz. Following sonication, the samples were centrifuged at 13,000 x g for 10 min at 4˚C. Subsequently, the supernatant (100 μg) was pre-absorbed by 50 μl protein G beads and was incubated with magnetic beads conjugated to 5 μg ETV4 antibody (1/200; cat. no. 65763; Cell Signaling Technology), Next, the mixture was washed with eluate buffer. The cross-linking was reversed by 5 M NaCl followed by incubation at 65˚C overnight. The precipitated DNA was analyzed by PCR to amplify the ETV4 binding site.

The results were normalized to the DNA precipitated by 5 μg IgG (1/100; cat. no. ab172730; Abcam).

RNA extraction and reverse transcription-quantitative PCR (RT-qPCR). The concentration of total RNA isolated from $1x10^6$ MCF10A and BC cell lines using TRIzol (Invitrogen; Thermo Fisher Scientific, Inc.) was quantified using a NanoDrop 3000 spectrophotometer (Thermo Fisher Scientific, Inc.). RNA was reverse-transcribed into cDNA using PrimeScript RT Master Mix (Takara Bio, Inc.) at 25˚C for 5 min, 42˚C for 30 min, 85˚C for 5 min and 4˚C for 5 min. qPCR was performed using SYBR Premix Ex Taq™ II kit (Takara Bio, Inc.). The thermocycling conditions were as follows: Initial denaturation at 95˚C for 3 min, followed by 35 cycles of 95˚C for 30 sec, 60˚C for 30 sec and 72˚C for 1 min, with final extension step at 72˚C for 7 min. The following primer pairs were used for qPCR: SLC12A5 forward (F), 5'-TCCCTCCTAGAGCCTGGTTG-3' and reverse (R), 5'-TTGGGGTTGCCATCACCTTT-3'; ETV4 F, 5'-GAAAAACAAGTCGGTGCGCT-3' and R, 5'-TTGCTG CTGAAGGTGTAGGG-3' and GAPDH F, 5'-GGGAAACTG TGGCGTGAT-3' and R, 5'-GAGTGGGTGTCGCTGTTG A-3'. mRNA level was quantified using the $2^{-\Delta\Delta Cq}$ method (29) and normalized to the internal reference gene GAPDH.

Western blot assay. The isolation of total protein from sample MCF10A and BC cell lines was conducted using RIPA buffer (Auragene Bioscience Co.) and the proteins were quantified using the bicinchoninic acid assay (Beyotime Institute of Biotechnology). Following separation by 10% SDS-PAGE (Bio-Rad Laboratories, Inc.), proteins (30 μg) were transferred to PVDF membranes (MilliporeSigma). The membranes were blocked with 5% skimmed milk in 0.1% tris-buffered saline with Tween-20 for 1 h at room temperature, then incubated with primary antibodies against SLC12A5 (1:1,000; cat. no. ab259969; Abcam), SLC7A11 (1:1,000; cat. no. ab175186; Abcam), glutathione peroxidase 4 (GPX4; 1:1,000; cat. no. ab125066; Abcam), acyl-CoA synthetase long chain family member 4 (ACSL4; 1:1,000; cat. no. ab205197, Abcam), transferrin receptor 1 (TFR1; 1:1,000; cat. no. ab109259; Abcam), ETV4 (1:1,000; cat. no. ab70425; Abcam) and β-actin (1:1,000, cat. no. ab8227; Abcam) overnight at 4˚C, followed by incubation with HRP-conjugated goat anti-rabbit (1:5,000; cat. no. sc-2004; Santa Cruz Biotechnology, Inc.) or anti-mouse secondary antibodies (1:5,000; cat. no. sc-2005; Santa Cruz Biotechnology, Inc.) for 1 h at room temperature. The protein bands were visualized using Amersham ECL Prime Western blotting detection reagent (Cytiva) in accordance with the manufacturer's instructions. Protein expression was quantified using ImageJ software (version 1.49; National Institutes of Health).

Statistical analysis. The data were analyzed using SPSS 23.0 software (IBM Corp.) and presented as the mean ± standard deviation from at least three independent experiments. For the comparison of multiple groups, one-way ANOVA followed by Bonferroni's post hoc test was used, while unpaired Student's t-test was applied for two groups. $P<0.05$ was considered to indicate a statistically significant difference.

Results

SLC12A5 is upregulated in BC tissue and cells. To evaluate the biological role of SLC12A5 in BC, SLC12A5 expression in BC tissue and cells was initially assessed. The results from the UALCAN database demonstrated that SLC12A5 expression was notably increased in tissues from patients with BC compared with normal tissues (Fig. 1A). Similarly, high expression of SLC12A5 in BC tissues was associated with worse prognosis, compared with patients with low/medium SLC12A5 expression according to the UALCAN database (Fig. 1B). Moreover, RT-qPCR and western blotting demonstrated that the mRNA and protein expression levels of SLC12A5 were both significantly increased in BC cell lines including MCF7, Hs578T, T47D and BT-549 cells compared with the normal mammary epithelial cell line MCF10A (Fig. 1C and D). As MCF-7 cells had a notably higher SLC12A5 expression than the other BC cell lines assessed, this cell line was used for further experiments. CCLE data also demonstrated that MCF-7 cells had the highest SLC12A5 mRNA expression of these cell lines (Fig. 1E).

SLC12A5 knockdown attenuates proliferation, migration and invasion of MCF-7 cells. To evaluate the biological role of SLC12A5 in BC cells, SLC12A5 expression was knocked down by transfection with sh-SLC12A5-1/2 (Fig. 2A and B). sh-SLC12A5-1 had a greater knockdown effect and was selected for subsequent assays. MCF-7 cell proliferation was significantly reduced following SLC12A5 knockdown compared with the sh-NC group (Fig. 2C). The colony formation assay also demonstrated that the number of cell colonies was notably decreased by sh-SLC12A5-1 transfection compared with sh-NC group (Fig. 2D). Furthermore, wound healing assay demonstrated that cell migration decreased in cells transfected with sh-SLC12A5-1 (Fig. 2E). Also, Transwell assay demonstrated that the number of invaded cells was significantly reduced when SLC12A5 was down-regulated (Fig. 2F).

SLC12A5 knockdown alleviates ferroptosis resistance in MCF-7 cells. To evaluate the effects of SLC12A5 knockdown on ferroptosis resistance in BC cells, TBARS assay was conducted. SLC12A5 knockdown significantly increased production of TBARS in MCF-7 cells compared with the sh-NC group (Fig. 3A). Furthermore, the levels of oxidized C11 were markedly increased while the levels of non-oxidized C11 were reduced following the knockdown of SLC12A5 (Fig. 3B). Moreover, SLC12A5 knockdown led to increased levels of Fe^{2+} (Fig. 3C). Similarly, western blotting demonstrated that levels of ferroptosis-related proteins SLC7A11 and GPX4 significantly decreased, whereas levels of ASCL4 and TFR1 significantly increased in SLC12A5-knockdown cells compared with the sh-NC group (Fig. 3D).

Knockdown of SLC12A5 inhibits reprogramming of glucose metabolism in MCF-7 cells. Transfection with sh-SLC12A5 decreased ECAR compared with the NC group (Fig. 4A). Moreover, SLC12A5 knockdown markedly increased OCR in MCF-7 cells compared with the sh-NC group (Fig. 4B). Moreover, knockdown of SLC12A5 significantly repressed

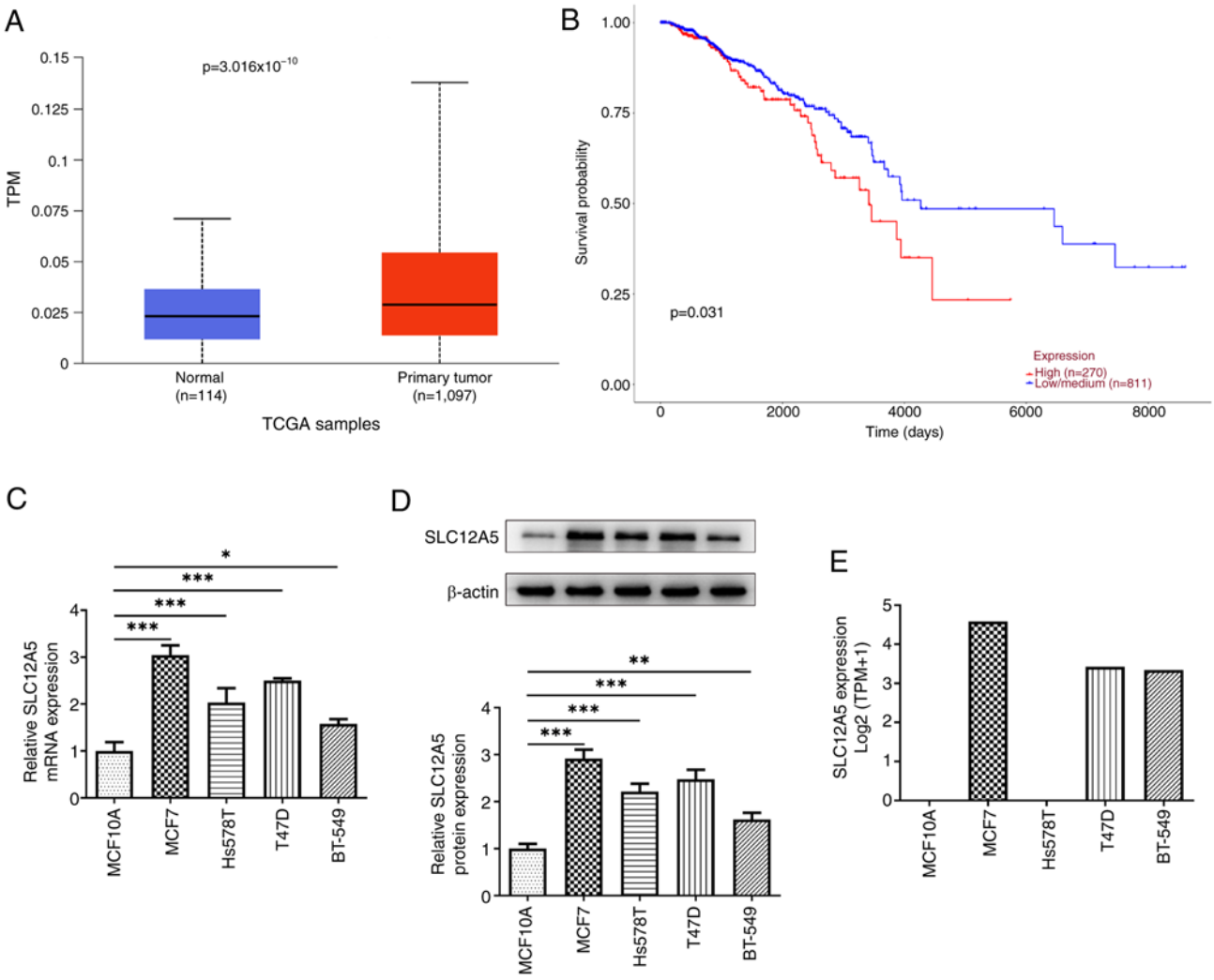

Figure 1. SLC12A5 is upregulated in BC tissues and cells. UALCAN database demonstrated (A) upregulation of SLC12A5 in BC tissues and (B) association between SLC12A5 upregulation and poor prognosis of patients with BC. The mRNA (C) and protein levels (D) of SLC12A5 in normal mammary epithelial cell line MCF10A and BC cells were detected using reverse transcription-quantitative PCR and western blot. (E) SLC12A5 expression in BC cell lines by The Cancer Cell Line Encyclopedia. *P<0.05, **P<0.01 and ***P<0.001. BC, breast cancer; TCGA, The Cancer Genome Atlas; SLC12A5, solute carrier family 12 member 5; TPM, transcript per million; UALCAN, University of ALabama at Birmingham CANcer data analysis Portal.

lactate release (Fig. 4C). Also, down-regulation of SLC12A5 reduced glucose uptake (Fig. 4D).

ETV4 transcription factor binds to SLC12A5 promoter and upregulates SLC12A5 expression. Both ETV4 mRNA and protein expression were significantly increased in MCF-7 cells compared with MCF10A cells (Fig. 5A and B). To identify the role of ETV4 in BC cells, oe-ETV4 and ETV4-knockdown plasmids were transfected into MCF-7 cells. The transfection efficiency was assessed using RT-qPCR and western blotting, which demonstrated that the ETV4 mRNA and protein expression significantly increased in the oe-EVT4 group compared with the oe-NC group (Fig. 5C and D). sh-ETV4-1 had a greater knockdown effect and was selected for the following assays (named as sh-ETV4-1). There was a significant increase in SLC12A5 expression following ETV4 overexpression and a significant decrease in SLC12A5 mRNA and protein expression following ETV4 knockdown compared with the corresponding NC (Fig. 5E and F). To verify the interaction between ETV4 and SLC12A5, the binding site of ETV4 on the SLC12A5 promoter sequence was predicted using HumanTFDB database (SLC12A5 WT: CTCCACTCACTCTCTTCCAGACACAATG; SLC12A5 MUT: CTCACAGACAGAGAGGAACTCACACATG) (Fig. 5G). Moreover, luciferase reporter assay demonstrated that the luciferase activity in SLC12A5-WT cells was significantly increased by ETV4 overexpression compared with oe-NC group, while no significant change in luciferase activity was observed in the SLC12A5-MUT groups with ETV4 overexpression (Fig. 5H). ChIP assay also demonstrated a significant enrichment of SLC12A5 in the ETV4 group compared with the IgG group (Fig. 5I).

Overexpression of ETV4 partially reverses the inhibitory effect of SLC12A5 knockdown on migration, invasion, ferroptosis resistance and glucose metabolism of BC cells. The role of ETV4 in SLC12A5-modulated migration and invasion, ferroptosis resistance and glucose metabolism in MCF-7 cells was determined. CCK-8 assay demonstrated that in SLC12A5-silencing cells, co-transfection of sh-SLC12A5-1 and oe-ETV4 increased cell proliferation rate again (Fig. 6A).

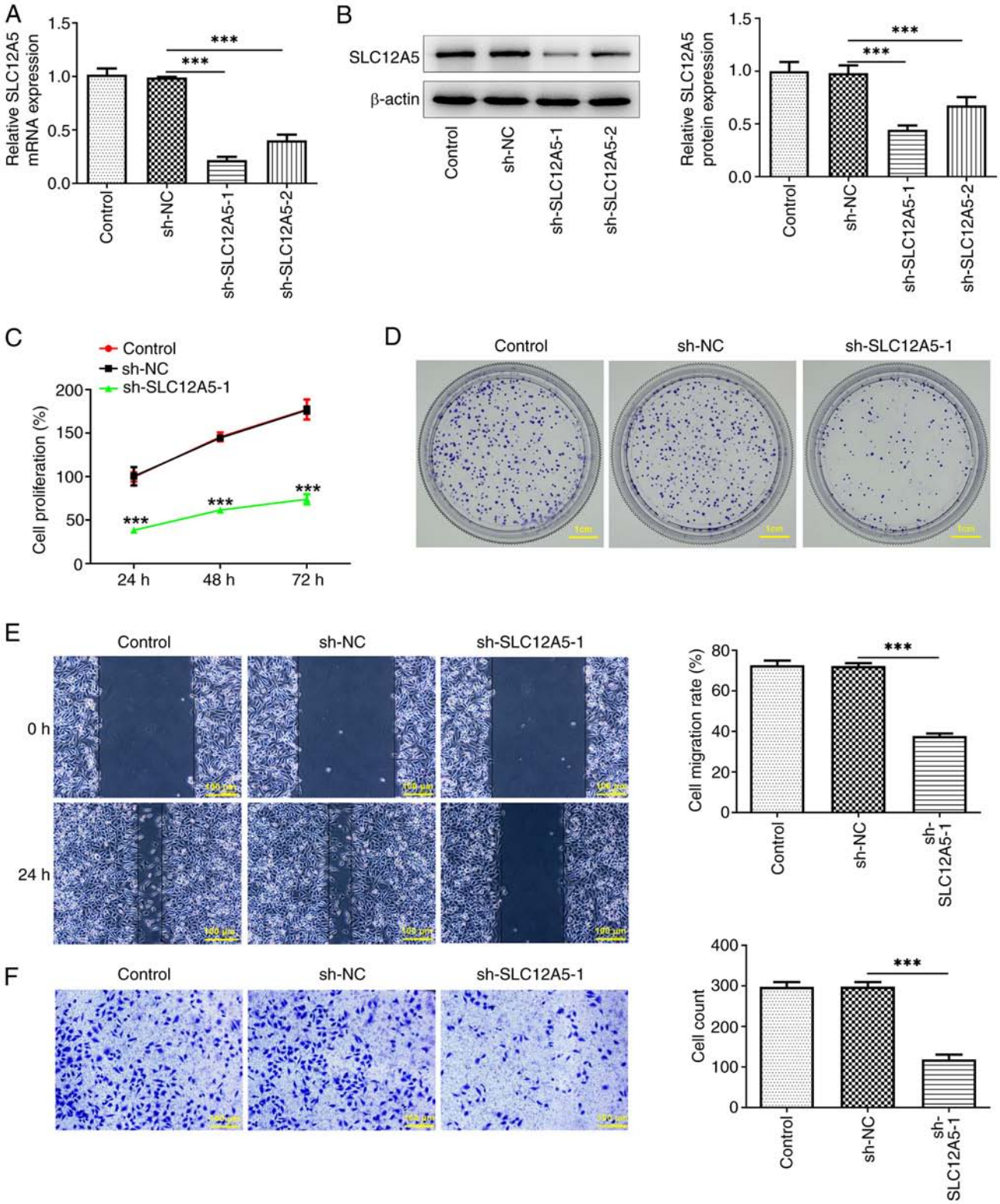

Figure 2. SLC12A5 knockdown attenuates proliferation, migration, invasion of MCF-7 cells. (A) mRNA and (B) protein levels of SLC12A5 in MCF-7 cells were measured using reverse transcription-quantitative PCR and western blotting following transfection with sh-SLC12A5. Cell proliferation was measured by (C) Cell Counting Kit-8 and (D) colony formation assay. (E) Wound healing assay was performed to assess cell migration. (F) Transwell assay was used to detect cell invasion. Magnification x100. ***P<0.001 compared with sh-NC. sh, short hairpin; NC, negative control; SLC12A5, Solute carrier family 12 member 5.

Colony formation assay demonstrated that relative to the sh-SLC12A5-1 + oe-NC group, concurrent down-regulation of SLC12A5 and overexpression of ETV4 enhanced the colony numbers (Fig. 6B). The reduced cell migration rate caused by SLC12A5 knockdown was enhanced again by co-transfection of sh-SLC12A5-1 and oe-ETV4 (Fig. 6C). Cell invasion ability was weakened in SLC12A5-depleting cells and was promoted again by further ETV4 overexpression (Fig. 6C and D).

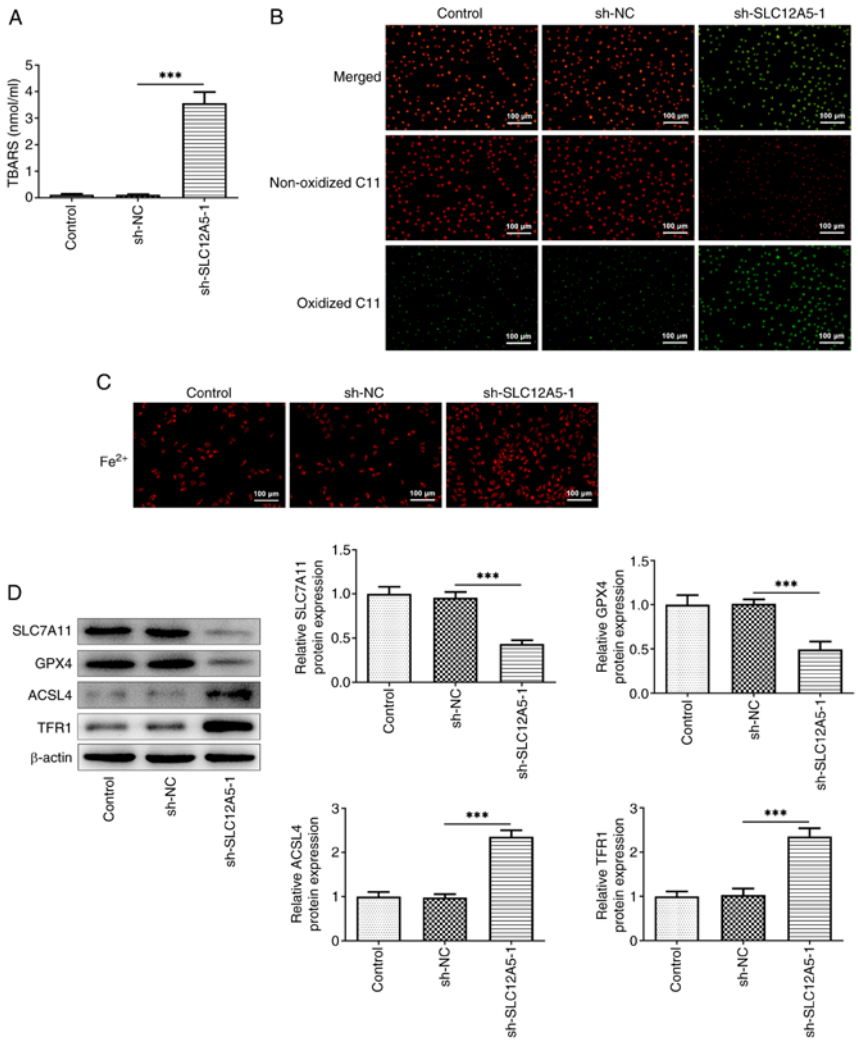

Figure 3. SLC12A5 knockdown alleviates ferroptosis resistance in MCF-7 cells. (A) TBARS assay and (B) C11 BODIPY 581/591 probe were used to assess lipid peroxidation. (C) Levels of Fe^{2+} in MCF-7 cells with or without transfection with sh-SLC12A5. Magnification, x100. (D) Western blotting was used to evaluate protein levels of SLC7A11, GPX4, ACSL4 and TFR1. ***P<0.001. TBARS, thiobarbituric acid reactive substances; sh, short hairpin; NC, negative control; SLC12A5, solute carrier family 12 member 5; GPX4, glutathione peroxidase 4; ACSL4, Acyl-CoA synthetase long-chain family 4; TFR1, transferrin receptor 1.

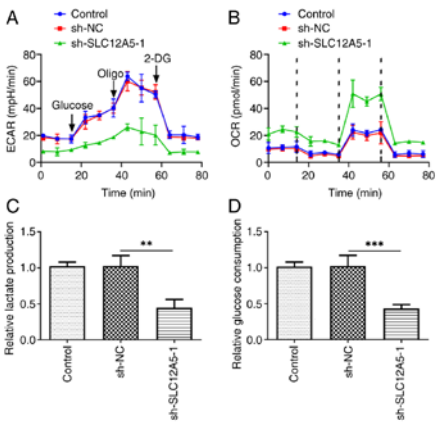

Figure 4. Knockdown of SLC12A5 inhibits reprogramming of glucose metabolism in MCF-7 cells. (A) ECAR, (B) OCR, (C) lactic acid production and (D) glucose consumption in MCF-7 cells with or without transfection with sh-SLC12A5 were assessed. **P<0.01 and ***P<0.001. ECAR, extracellular acidification rate; OCR, oxygen consumption rate; sh, short hairpin; NC, negative control; SLC12A5, solute carrier family 12 member 5; oligo, oligonucleotide; 2-DG, 2-deoxyglucose.

Furthermore, overexpression of ETV4 significantly decreased the production of TBARS (Fig. 7A) and notably decreased the levels of Fe^{2+} (Fig. 7C) compared with SLC12A5-knockdown cells without ETV4 overexpression. Moreover, an increase in red fluorescence and a decrease in green fluorescence was observed in MCF-7 cells co-transfected with sh-SLC12A5-1 and oe-ETV4 compared with sh-SLC12A5-1 alone (Fig. 7B). Consistently, ETV4 overexpression significantly increased protein levels of SLC7A11 and GPX4 and significantly decreased protein levels of ASCL4 and TFR1 compared with SLC12A5 knockdown alone (Fig. 7D). Finally, further overexpression of ETV4 increased the ECAR in SLC12A5-silencing cells (Fig. 8A). Compared with the sh-SLC12A5-1 + oe-NC group, OCR value was decreased in the sh-SLC12A5-1 + oe-ETV4 group (Fig. 8B). Also, SLC12A5 knockdown inhibited lactate production, which was partially reversed by further up-regulation of ETV4 (Fig. 8C). Similarly, overexpression of ETV4 promoted glucose consumption that was declined in cells transfected with sh-SLC12A5-1 (Fig. 8D).

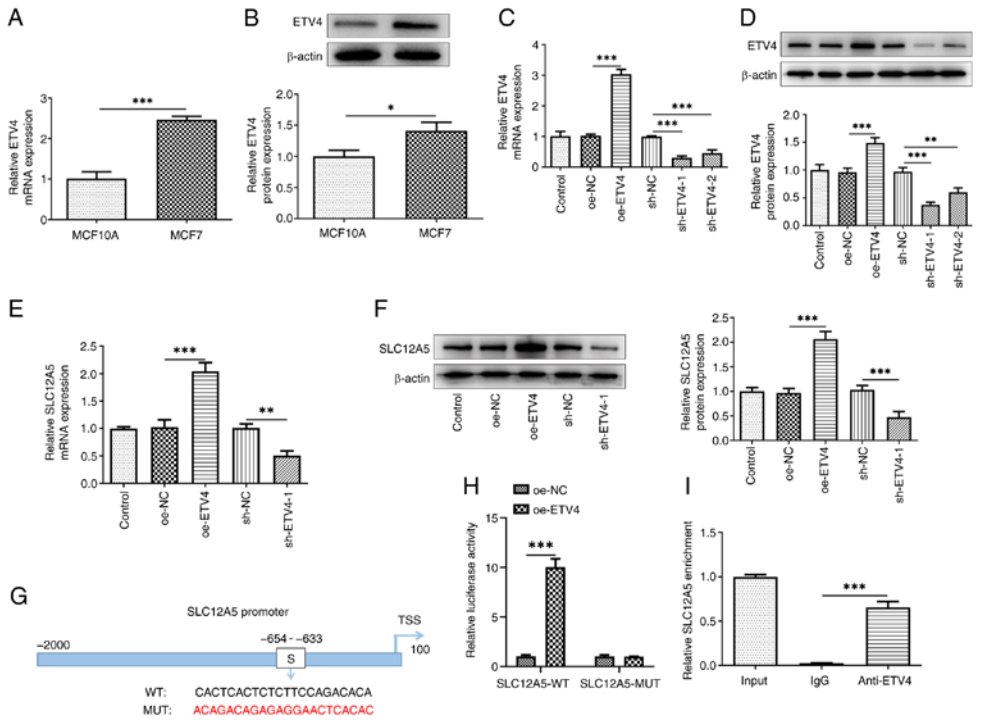

Figure 5. Transcription factor ETV4 binds to SLC12A5 promoter and upregulates SLC12A5 expression. (A) mRNA and (B) protein levels of ETV4 in normal mammary epithelial cell line MCF10A and MCF-7 cells were measured using RT-qPCR and western blotting. (C) mRNA and (D) protein levels of ETV4 and (E) mRNA and (F) protein levels of SLC12A5 were detected by RT-qPCR and western blotting in MCF-7 cells after ETV4 was overexpressed or knocked down. (G) Binding site of ETV4 and SLC12A5 promoter. (H) SLC12A5 promoter activity was evaluated by luciferase reporter assay. (I) Chromatin immunoprecipitation assay was performed to detect the binding of ETV4 to the WT and MUT SLC12A5 promotor. *P<0.05, **P<0.01 and ***P<0.001. sh, short hairpin; NC, negative control; oe, overexpression; WT, wild-type; MUT, mutant; RT-qPCR, reverse transcription-quantitative PCR; sh, short hairpin; NC, negative control; SLC12A5, solute carrier family 12 member 5; TSS, transcription start site; ETV4, E-twenty-six-specific sequence variant 4.

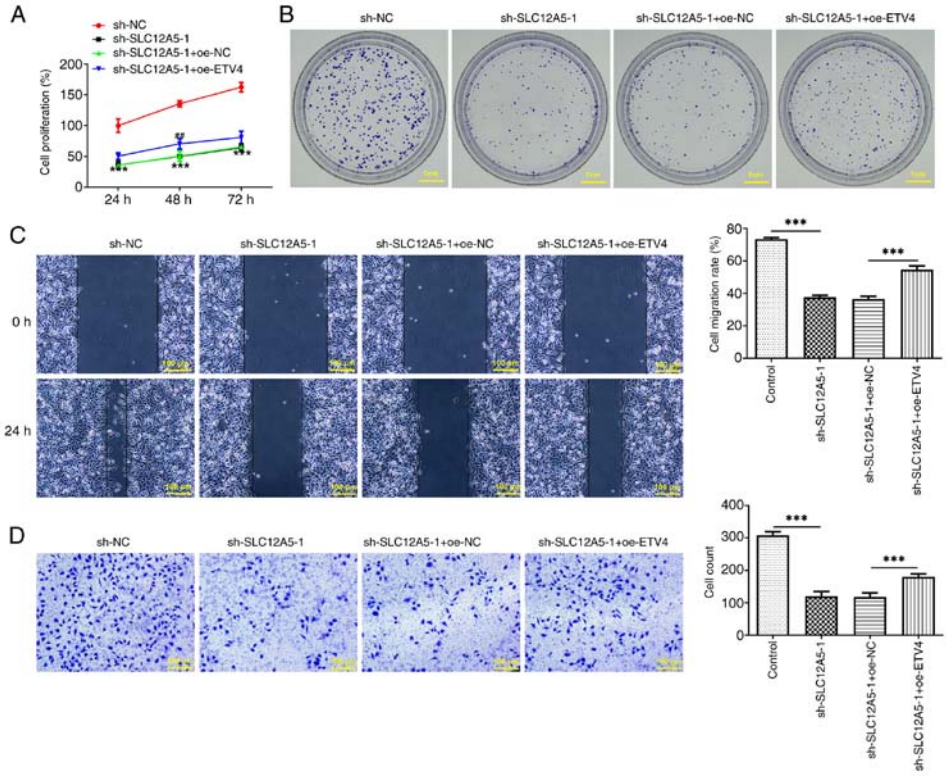

Figure 6. Overexpression of ETV4 partially reverses the inhibitory effect of SLC12A5 knockdown on the migration and invasion of breast cancer cells. Cell proliferation was identified by (A) Cell Counting Kit-8 (***P<0.001 vs. Control; $^{\#\#}$P<0.01 compared with sh-SLC12A5 + oe-NC) and (B) colony formation assay. (C) Wound healing assay was performed to assess cell migration. (D) Transwell assay was used to detect cell invasion. Magnification, x100. ***P<0.001 compared with Control or sh-SLC12A5 + oe-NC. sh, short hairpin; NC, negative control; oe, overexpression; ETV4, E-twenty-six-specific sequence variant 4; SLC12A5, Solute carrier family 12 member 5.

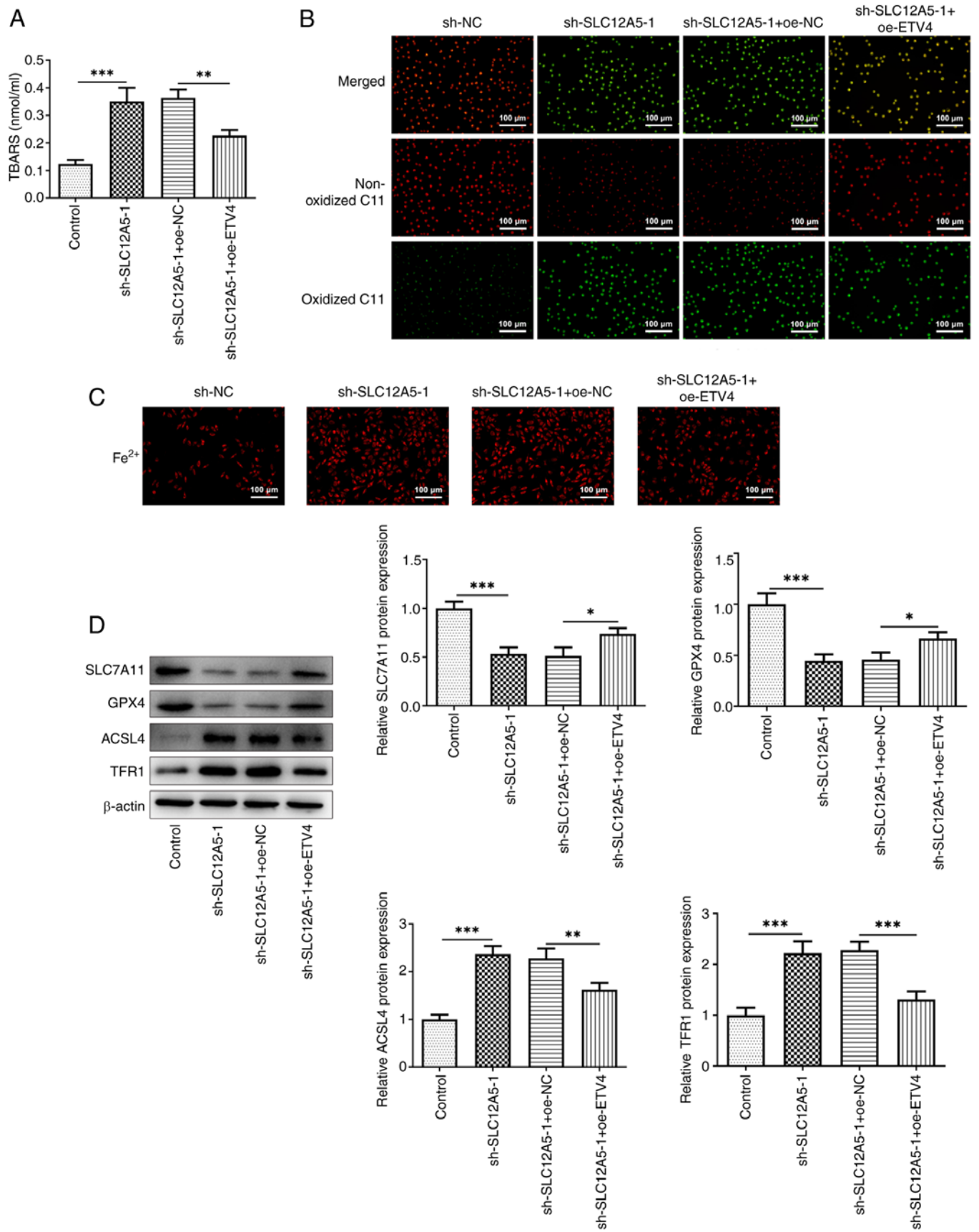

Figure 7. Overexpression of ETV4 partially reverses the inhibitory effect of SLC12A5 knockdown on ferroptosis resistance of BC cells. (A) TBARS assay and (B) C11 BODIPY 581/591 probe were used to assess lipid peroxidation. (C) Levels of Fe^{2+} in MCF-7 cells transfected with sh-SLC12A5 with or without oe-ETV4. Magnification, x100. (D) Western blotting was used to evaluate protein levels of SLC7A11, GPX4, ACSL4 and TFR1. $^{*}P<0.05$, $^{**}P<0.01$ and $^{***}P<0.001$. TBARS, thiobarbituric acid reactive substances; sh, short hairpin; NC, negative control; oe, overexpression; ETV4, E-26-specific sequence variant 4; SLC12A5, solute carrier family 12 member 5; GPX4, glutathione peroxidase 4; ACSL4, Acyl-CoA synthetase long-chain family 4; TFR1, transferrin receptor 1.

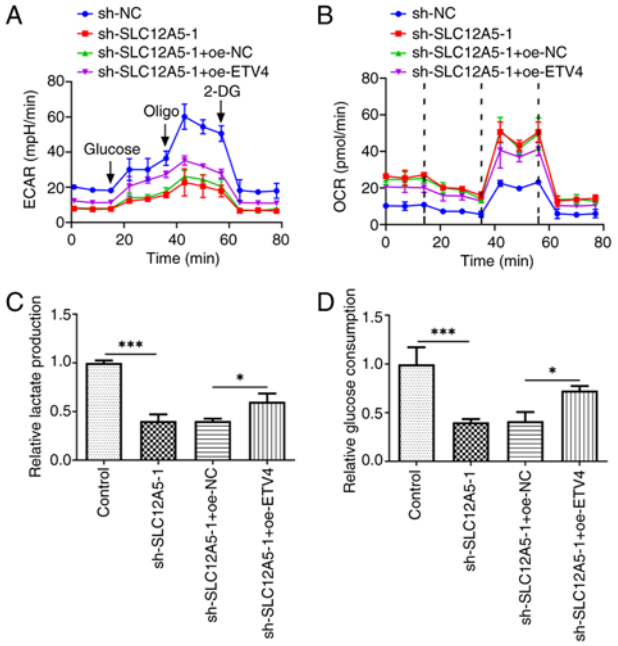

Figure 8. Overexpression of ETV4 partially reverses the inhibitory effect of SLC12A5 silencing on glucose metabolism of BC cells. (A) ECAR, (B) OCR, (C) lactic acid production and (D) glucose consumption in MCF-7 cells transfected with sh-SLC12A5 with or without oe-ETV4 were assessed. *P<0.05 and ***P<0.001. ECAR, extracellular acidification rate; OCR, oxygen consumption rate; sh, short hairpin; NC, negative control; ETV4, E-twenty-six-specific sequence variant 4; SLC12A5, Solute carrier family 12 member 5; 2-DG, 2-deoxyglucose; oligo, oligonucleotide.

Discussion

BC is the most commonly diagnosed malignancy in female patients worldwide and the second highest contributor to cancer-related mortality in female patients (30). The incidence and mortality rates of BC continue to rise worldwide, posing a threat to the physical and mental health and lives of patients (31). Hence, early diagnosis and monitoring of BC is key. The demand for identification of effective biomarkers for BC, particularly novel molecular therapeutic targets, has been highlighted (32). In the present study, it was demonstrated that SLC12A5 was upregulated in BC tissue and cells and ETV4 was overexpressed in BC cells and high SLC12A5 expression was positively associated with poor prognosis in patients with BC. SLC12A5 knockdown ameliorated MCF-7 cell proliferation, migration, ferroptosis resistance and glucose metabolism reprogramming. Moreover, ETV4 overexpression promoted SLC12A5 transcription and ETV4 overexpression reversed the anticancer effects of SLC12A5 knockdown in MCF-7 cells.

SLC12A5 can promote intracellular transport of K^+ and Cl^- ions (33). Previous studies have shown that SLC12A5 expression is elevated in numerous tumor types and high expression is typically associated with a poor prognosis (34,35). Yang *et al* (36) reported that FEZF1 antisense RNA 1 (FEZF1-AS1) is highly expressed in cervical cancer (CC) cells and that increased levels of FEZF1-AS1 increases the proliferation, migration and invasion capabilities of CC cells. FEZF1-AS1 also decreases apoptosis via the microRNA-367-3p/SLC12A5 signaling axis. Another study reported that high expression of SLC12A5 protein indicates an aggressive and/or invasive phenotype in ovarian cancer (37). In the present study, SLC12A5 was increased in BC tissues and was associated with poor prognosis according to the analysis of data from the UALCAN database. Increased SLC12A5 expression in BC cell lines was verified by *in vitro* experiments.

HumanTFDB website was used to evaluate the upstream and downstream mechanisms of SLC12A5. Numerous transcription factors are reported to bind to the SLC12A5 promoter, among which only ETV4 is reported to be associated with ferroptosis resistance and glucose metabolic reprogramming (24,38). Therefore, the role of ETV4 was further assessed. Yuan *et al* (39) reported that high ETV4 expression increases the risk of distant metastasis in patients with triple-negative BC, leading to poor prognosis. Furthermore, ETV4 facilitates the proliferation, migration, invasion and anchorage-independent growth of mammary tumors in mice (40). In the present study, it was demonstrated that ETV4 expression was elevated in BC compared with the control cells. To evaluate the interaction between ETV4 and SLC12A5, the binding site of ETV4 in the SLC12A5 promoter was predicted using the HumanTFDB database and confirmed experimentally by luciferase reporter and ChIP assays.

Wang *et al* (38) reported that ETV4 knockdown facilitates ferroptosis to inhibit the progression of papillary thyroid carcinoma through the downregulation of SLC7A11. Verma *et al* (41) used RNA sequencing to evaluate the role of genes in the metabolic reprogramming and drug resistance of prostate cancer; upregulation of SLC12A5 was associated with higher lactate/citrate uptake and lower glucose uptake in drug-resistant cells. In human BC tissues, ETV4 expression is associated with the glycolytic signaling pathway and ETV4 deficiency markedly suppresses the expression of glycolytic enzymes such as hexokinase 2 and lactate dehydrogenase A and decreases glucose uptake and lactate release in BC cells (24). Similarly, the present study demonstrated that SLC12A5 knockdown in MCF-7 cells promoted ferroptosis and decreased glucose metabolism reprogramming, which were reversed following overexpression of ETV4.

However, the present experiments were performed in cell lines only, with no verification from patient samples. Moreover, the association between the expression of SLC12A5 and ETV4 in BC and healthy controls should be assessed. Future studies should assess the SLC12A5 expression by immunofluorescence staining, immunohistochemistry staining and evaluate the association between SLC12A5 and ETV4 in clinical samples. Tumor microenvironment, including immune cell infiltration, serves a role in cancer progression and outcomes (42). It is possible that the role of SLC12A5 may exert an effect on immune filtration. Thus, the association between SLC12A5 expression and immune cell infiltration in BC should be assessed.

In conclusion, the present study reported a mechanism of SLC12A5 regulated by ETV4 in BC cells, which may serve a role in ferroptosis and glucose metabolism. The present study may therefore contribute to the understanding of BC pathogenesis and offer prospective therapeutic targets for patients with BC.

Acknowledgements

Not applicable.

Funding

No funding was received.

Availability of data and materials

The data generated in the present study may be requested from the corresponding author.

Authors' contributions

HW and FW designed the study and wrote and revised the manuscript. HW and YD analyzed the data and searched the literature. All authors performed experiments. HW and FW confirm the authenticity of all the raw data. All authors have read and approved the final manuscript.

Ethics approval and consent to participate

Not applicable.

Patient consent for publication

Not applicable.

Competing interests

The authors declare that they have no competing interests.

References

1. Zannetti A: Breast cancer: From pathophysiology to novel therapeutic Approaches 2.0. Int J Mol Sci 24: 2542, 2023.
2. Siegel RL, Giaquinto AN and Jemal A: Cancer statistics, 2024. CA Cancer J Clin 74: 12-49, 2024.
3. Houghton SC and Hankinson SE: Cancer progress and priorities: Breast cancer. Cancer Epidemiol Biomarkers Prev 30: 822-844, 2021.
4. De Rose F, Meduri B, De Santis MC, Ferro A, Marino L, Colciago RR, Gregucci F, Vanoni V, Apolone G, Di Cosimo S, *et al*: Rethinking breast cancer follow-up based on individual risk and recurrence management. Cancer Treat Rev 109: 102434, 2022.
5. Parisi S, Gambardella C, Conzo G, Ruggiero R, Tolone S, Lucido FS, Iovino F, Fisone F, Brusciano L, Parmeggiani D and Docimo L: Advanced localization technique for non-palpable breast cancer: Radiofrequency alone VS combined technique with ultrasound. J Clin Med 12: 5076, 2023.
6. Parisi S, Ruggiero R, Gualtieri G, Volpe ML, Rinaldi S, Nesta G, Bogdanovich L, Lucido FS, Tolone S, Parmeggiani D, *et al*: Combined LOCalizer™ and intraoperative ultrasound localization: First experience in localization of non-palpable breast cancer. In Vivo 35: 1669-1676, 2021.
7. Kawiak A: Molecular research and treatment of breast cancer. Int J Mol Sci 23: 9617, 2022.
8. Jiang X, Stockwell BR and Conrad M: Ferroptosis: Mechanisms, biology and role in disease. Nat Rev Mol Cell Biol 22: 266-282, 2021.9.
9. Chen X, Kang R, Kroemer G and Tang D: Broadening horizons: The role of ferroptosis in cancer. Nat Rev Clin Oncol 18: 280-296, 2021.
10. Liu J, Kang R and Tang D: Signaling pathways and defense mechanisms of ferroptosis. Febs J 289: 7038-7050, 2022.
11. Sun S, Shen J, Jiang J, Wang F and Min J: Targeting ferroptosis opens new avenues for the development of novel therapeutics. Signal Transduct Target Ther 8: 372, 2023.
12. Li Z, Chen L, Chen C, Zhou Y, Hu D, Yang J, Chen Y, Zhuo W, Mao M, Zhang X, *et al*: Targeting ferroptosis in breast cancer. Biomark Res 8: 58, 2020.
13. Fukuda A and Watanabe M: Pathogenic potential of human SLC12A5 variants causing KCC2 dysfunction. Brain Res 1710: 1-7, 2019.
14. Damanskienė E, Balnytė I, Valančiūtė A, Alonso MM and Stakišaitis D: Different effects of valproic acid on SLC12A2, SLC12A5 and SLC5A8 gene expression in pediatric glioblastoma cells as an approach to personalised therapy. Biomedicines 10: 968, 2022.
15. Jiang Y, Liao HL and Chen LY: A pan-cancer analysis of SLC12A5 reveals its correlations with tumor immunity. Dis Markers 2021: 3062606, 2021.
16. .Yuan S, He SH, Li LY, Xi S, Weng H, Zhang JH, Wang DQ, Guo MM, Zhang H, Wang S, *et al*: A potassium-chloride co-transporter promotes tumor progression and castration resistance of prostate cancer through m(6)A reader YTHDC1. Cell Death Dis 14: 7, 2023.
17. Peng L, Cao Z, Wang Q, Fang L, Yan S, Xia D, Wang J and Bi L: Screening of possible biomarkers and therapeutic targets in kidney renal clear cell carcinoma: Evidence from bioinformatic analysis. Front Oncol 12: 963483, 2022.
18. Tong Q, Qin W, Li ZH, Liu C, Wang ZC, Chu Y and Xu XD: SLC12A5 promotes hepatocellular carcinoma growth and ferroptosis resistance by inducing ER stress and cystine transport changes. Cancer Med 12: 8526-8541, 2023.
19. Wang L, Zhang Q, Wu P, Xiang W, Xie D, Wang N, Deng M, Cao K, Zeng H, Xu Z, *et al*: SLC12A5 interacts and enhances SOX18 activity to promote bladder urothelial carcinoma progression via upregulating MMP7. Cancer Sci 111: 2349-2360, 2020.
20. Singh R, Dagar P, Pal S, Basu B and Shankar BS: Significant alterations of the novel 15 gene signature identified from macrophage-tumor interactions in breast cancer. Biochim Biophys Acta Gen Subj 1862: 669-683, 2018.
21. Neri P, Barwick BG, Jung D, Patton JC, Maity R, Tagoug I, Stein CK, Tilmont R, Leblay N, Ahn S, *et al*: ETV4-dependent transcriptional plasticity maintains MYC expression and results in IMiD resistance in multiple myeloma. Blood Cancer Discov 5: 56-73, 2024.
22. Qi D, Lu M, Xu P, Yao X, Chen Y, Gan L, Li Y, Cui Y, Tong X, Liu S, *et al*: Transcription factor ETV4 promotes the development of hepatocellular carcinoma by driving hepatic TNF-α signaling. Cancer Commun (Lond) 43: 1354-1372, 2023.
23. Cosi I, Moccia A, Pescucci C, Munagala U, Di Giorgio S, Sineo I, Conticello SG, Notaro R and De Angioletti M: Identification and characterization of novel ETV4 splice variants in prostate cancer. Sci Rep 13: 5267. 2023.
24. Zhu T, Zheng J, Zhuo W, Pan P, Li M, Zhang W, Zhou H, Gao Y, Li X and Liu Z: ETV4 promotes breast cancer cell stemness by activating glycolysis and CXCR4-mediated sonic Hedgehog signaling. Cell Death Discov 7: 126, 2021.
25. Liu B, Zhang J, Meng X, Xie SM, Liu F, Chen H, Yao D, Li M, Guo M, Shen H, *et al*: HDAC6-G3BP2 promotes lysosomal-TSC2 and suppresses mTORC1 under ETV4 targeting-induced low-lactate stress in non-small cell lung cancer. Oncogene 42: 1181-1195, 2023.
26. Chandrashekar DS, Bashel B, Balasubramanya SA, Creighton CJ, Ponce-Rodriguez I, Chakravarthi BVSK and Varambally S: A portal for facilitating tumor subgroup gene expression and survival analyses. Neoplasia 19: 649-658, 2017.27.
27. Hu H, Miao YR, Jia LH, Yu QY, Zhang Q and Guo AY: AnimalTFDB 3.0: A comprehensive resource for annotation and prediction of animal transcription factors. Nucleic Acids Res 47: D33-D38, 2019.28.
28. Nusinow DP, Szpyt J, Ghandi M, Rose CM, McDonald ER III, Kalocsay M, Jané-Valbuena J, Gelfand E, Schweppe DK, Jedrychowski M, *et al*: Quantitative proteomics of the cancer cell line encyclopedia. Cell 180: 387-402e16, 2020.
29. Livak KJ and Schmittgen TD: Analysis of relative gene expression data using real-time quantitative PCR and the 2(-Delta Delta C(T)) method. Methods 25: 402-408, 2001.
30. Trayes KP and Cokenakes SEH: Breast cancer treatment. Am Fam Physician 104: 171-178, 2021.
31. Zhang YN, Xia KR, Li CY, Wei BL and Zhang B: Review of breast cancer pathologigcal image processing. Biomed Res Int 2021: 1994764. 2021.
32. Criscitiello C and Corti C: Breast cancer genetics: Diagnostics and treatment. Genes (Basel) 13: 1593, 2022.

33. Kontou G, Josephine Ng SF, Cardarelli RA, Howden JH, Choi C, Ren Q, Rodriguez Santos MA, Bope CE, Dengler JS, Kelley MR, *et al*: KCC2 is required for the survival of mature neurons but not for their development. J Biol Chem 296: 100364, 2021.
34. Tang Y, Qing C, Wang J and Zeng Z: DNA methylation-based diagnostic and prognostic biomarkers for glioblastoma. Cell Transplant 29: 963689720933241, 2020.
35. Gao JL, Peng K, Shen MW, Hou YH, Qian XB, Meng XW, Ji FH, Wang LN and Yang JP: Suppression of WNK1-SPAK/OSR1 attenuates bone cancer pain by regulating NKCC1 and KCC2. J Pain 20: 1416-1428, 2019.
36. Yang X, Qu Y and Zhang J: Up-regulated LncRNA FEZF1-AS1 promotes the progression of cervical carcinoma cells via MiR-367-3p/SLC12A5 signal axis. Arch Med Res 53: 9-19, 2022.
37. Yang GP, He WP, Tan JF, Yang ZX, Fan RR, Ma NF, Wang FW, Chen L, Li Y, Li Y, *et al*: Overexpression of SLC12A5 is associated with tumor progression and poor survival in ovarian carcinoma. Int J Gynecol Cancer 29: 1280-1284, 2019.
38. Wang L, Zhang Y, Yang J, Liu L, Yao B, Tian Z and He J: The knockdown of ETV4 inhibits the papillary thyroid cancer development by promoting ferroptosis upon SLC7A11 down-regulation. DNA Cell Biol 40: 1211-1221, 2021.
39. Yuan ZY, Dai T, Wang SS, Peng RJ, Li XH, Qin T, Song LB and Wang X: Overexpression of ETV4 protein in triple-negative breast cancer is associated with a higher risk of distant metastasis. Onco Targets Ther 7: 1733-1742, 2014.
40. Dumortier M, Ladam F, Damour I, Vacher S, Bièche I, Marchand N, de Launoit Y, Tulasne D and Chotteau-Lelièvre A: ETV4 transcription factor and MMP13 metalloprotease are interplaying actors of breast tumorigenesis. Breast Cancer Res 20: 73, 2018.
41. Verma S, Shankar E, Chan ER and Gupta S: Metabolic reprogramming and predominance of solute carrier genes during acquired enzalutamide resistance in prostate cancer. Cells 9: 2535, 2020.
42. de Visser KE and Joyce JA: The evolving tumor microenvironment: From cancer initiation to metastatic outgrowth. Cancer Cell 41: 374-403, 2023.